Metabotropic NMDA receptor function is required for β-amyloid–induced synaptic depression

Helmut W. Kessels[a,b,1], Sadegh Nabavi[a,1], and Roberto Malinow[a,2]

[a]Center for Neural Circuits and Behavior, Departments of Neuroscience and Biology, University of California at San Diego, La Jolla, CA 92093; and [b]Netherlands Institute for Neuroscience, Royal Netherlands Academy of Arts and Sciences, 1105 BA, Amsterdam, The Netherlands

Contributed by Roberto Malinow, November 9, 2012 (sent for review September 27, 2012)

The mechanisms by which β-amyloid (Aβ), a peptide fragment believed to contribute to Alzheimer's disease, leads to synaptic deficits are not known. Here we find that elevated oligomeric Aβ requires ion flux-independent function of NMDA receptors (NMDARs) to produce synaptic depression. Aβ activates this metabotropic NMDAR function on GluN2B-containing NMDARs but not on those containing GluN2A. Furthermore, oligomeric Aβ leads to a selective loss of synaptic GluN2B responses, effecting a switch in subunit composition from GluN2B to GluN2A, a process normally observed during development. Our results suggest that conformational changes of the NMDAR, and not ion flow through its channel, are required for Aβ to produce synaptic depression and a switch in NMDAR composition. This Aβ-induced signaling mediated by alterations in GluN2B conformation may be a target for therapeutic intervention of Alzheimer's disease.

synapse | ion-flow independent | amyloid-beta | NR2A | NR2B

There is growing evidence that soluble oligomeric clusters of β-amyloid (Aβ), a secreted proteolytic derivative of the amyloid precursor protein (APP), are important for the early synaptic failure that is seen in Alzheimer's disease pathogenesis (1–5). An increased production of Aβ leads to synaptic depression, a loss of spines, and a reduced capacity for synaptic plasticity (6–14). However, the signaling pathways used by Aβ to cause its synapto-toxic effects are poorly understood. Several studies have shown that a blockade of NMDA receptors (NMDARs) can mitigate the effects of Aβ on synapses (3, 7, 10, 15–21). We sought to examine more carefully the role of NMDARs in the actions of oligomeric Aβ.

NMDARs are ionotropic receptors whose permeability for cations is controlled by a voltage-dependent Mg^{2+} block. NMDARs are tetramers consisting of two glycine-binding GluN1 and two glutamate-binding GluN2 subunits. In the postsynaptic membrane of hippocampal neurons two GluN2 isoforms dominate: GluN2A and GluN2B. Whereas GluN2B is predominant in synapses of the early postnatal brain, GluN2A numbers progressively increase with age and eventually outnumber GluN2Bs (22–25). This developmental switch from GluN2B- to GluN2A-rich synapses has important implications for the induction of NMDAR-mediated plasticity (26–29).

The activation of NMDARs is required for several forms of synaptic plasticity and learning (30–32). Ca^{2+} ion flow through the NMDAR can ignite multiple types of biochemical signaling (33, 34), and this is widely assumed to be the primary mechanism through which NMDARs control synaptic plasticity [see the companion article (35)]. However, an alternative NMDAR function, one that depends on glutamate binding but does not require ion flow through its channel, has been described to play a role in NMDAR endocytosis (36) and the NMDAR subunit switch (37). We here demonstrate that oligomeric Aβ generates synaptic depression and accelerates the NMDAR subunit switch, by modulating signaling pathways that depend on activation of the GluN2B subunit but do not depend on ion flux through the NMDAR.

Results

Aβ-Oligomers Cause Synaptic Depression. Elevated Aβ levels were achieved in organotypic hippocampal slice neurons by viral expression of APP-CT100, the β-secretase product of APP and precursor to Aβ (7). We compared evoked synaptic AMPA receptor (AMPAR) transmission between neighboring infected and uninfected CA1 neurons by paired whole-cell recordings (Fig. 1*A*). As previously shown (7), neurons in sparsely infected slices expressing APP-CT100 displayed depressed excitatory transmission (Fig. 1 *B* and *F*). Sparse infection is important because this ensures that synapses in control neurons will be sufficiently far from Aβ-producing infected neurons (7). Synaptic AMPAR depression was not observed in neurons expressing APP-CT84 (Fig. 1 *C* and *F*), the α-secretase product of APP, or in slices incubated during the APP-CT100 expression period with γ-secretase inhibitor L-685,458 (Fig. 1 *D* and *F*). These data indicate that synaptic AMPAR depression is caused by an increased production of Aβ by APP-CT100–expressing neurons. Synaptic depression was also significantly blocked by 5 μM *scyllo*-Inositol (Fig. 1 *E* and *F*), a drug that prevents the effects of oligomeric Aβ (38), suggesting that in our model system we study the effects of Aβ-oligomers on synapses.

Aβ-Driven Synaptic Depression Requires GluN2B Activation. To study the role of NMDAR activation in Aβ-mediated synaptic depression, slices were incubated during APP-CT100 expression with 100 μM D-(-)-2-Amino-5-phosphonopentanoic acid (D-APV, an NMDAR antagonist acting at the glutamate binding site on the GluN2 subunit). As previously shown (7), in D-APV–incubated slices the Aβ-mediated depressed transmission onto neurons expressing APP-CT100 was significantly reduced (D-APV vs. no drug: $P = 0.008$; Fig. 2 *A* and *C*). Similar results on Aβ-mediated synaptic depression were obtained with 20 μM 3-((*R*)-2-Carboxypiperazin-4-yl)-propyl-1-phosphonic acid (R-CPP), another antagonist for the GluN2 glutamate-binding site (R-CPP vs. no drug: $P = 0.02$; Fig. 2 *B* and *C*). These results verify that NMDAR activation is required for the depressive effects of Aβ-oligomers on synapses.

Recent studies have found that NMDAR antagonists targeting the GluN2B subunit can mitigate the effects of Aβ on synapses (15, 16, 18, 19). To study the role of the GluN2B subunit of the NMDAR in Aβ-mediated synaptic AMPAR depression, slices were incubated during APP-CT100 expression with either 3 μM Ro 25-6981 or 30 μM ifenprodil. Both drugs are activity-dependent antagonists that lock the GluN2B structure in a closed conformation (39). In slices incubated in antagonists targeting GluN2B, Aβ-driven synaptic depression was virtually abolished (Fig. 2 *D*, *E*, and *H*). These results indicate that oligomeric Aβ requires GluN2B activity to initiate AMPAR depression. The

Author contributions: H.W.K., S.N., and R.M. designed research; H.W.K. and S.N. performed research; H.W.K. and S.N. analyzed data; and H.W.K., S.N., and R.M. wrote the paper.

The authors declare no conflict of interest.

[1]H.W.K. and S.N. contributed equally to this work.

[2]To whom correspondence should be addressed. E-mail: rmalinow@ucsd.edu.

This article contains supporting information online at www.pnas.org/lookup/suppl/doi:10.1073/pnas.1219605110/-/DCSupplemental.

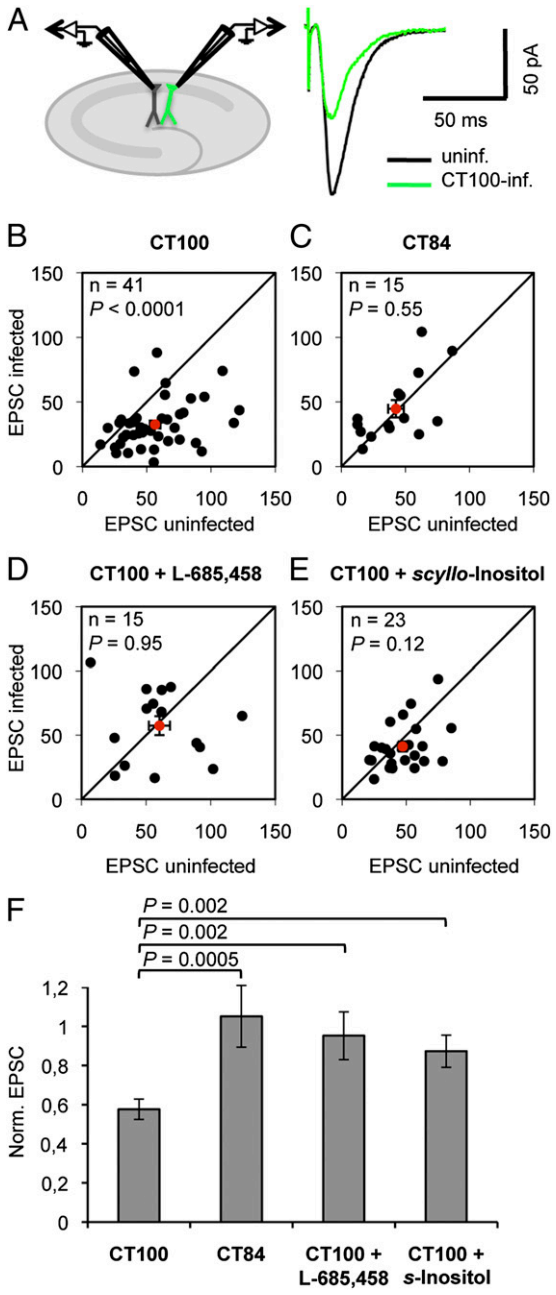

Fig. 1. APP-CT100–expressing neurons display oligomeric Aβ-mediated synaptic AMPAR depression. (*A*) Model figure for a dual whole-cell recording of an infected and a neighboring uninfected CA1 neuron (*Left*) and an example trace of evoked AMPAR currents of such a recording (*Right*). (*B–E*) Dot-plots of paired excitatory postsynaptic currents (EPSC) recordings, average (with error bars, SEM) denoted in red. (*F*) EPSCs of APP-CT100–infected neurons normalized to neighboring uninfected neurons upon incubation with indicated drugs. APP-CT100 (*B*), but not APP-CT84 expression (*C*) or incubation with the γ-secretase inhibitor L-685,458 (*D*), or incubation with 5 μM *scyllo*-Inositol (*E*), leads to synaptic AMPAR depression. Error bars, SEM. Statistics: paired Student *t* test of log-transformed data when comparing cell pairs (*B–E*), nonpaired Student *t* test when comparing different conditions (*F*).

GluN2B-selective antagonists (Ro 25-6981 and ifenprodil) tend to block Aβ-mediated synaptic depression more efficiently compared with the nonselective GluN2 antagonists (D-APV and R-CPP), suggesting that blockade of GluN2A does not contribute to this blockade. It is likely that the efficiency by which a drug inhibits the effects of Aβ depends on their inhibitory constants (K_i) to GluN2B: Aβ-driven synaptic depression was most effectively blocked when the antagonist had a greater affinity to GluN2B ($P = 0.03$; Fig. 2*F*). To determine whether the GluN2A subunit is necessary we used the drug ({[(1S)-1-(4-bromophenyl) ethyl]amino}-(2,3-dioxo-1,4-dihydroquinoxalin-5-yl)methyl)phosphonic acid (PEAQX), a competitive GluN2 antagonist that at a concentration of 50 nM blocks ∼80% of GluN2A currents and ∼20% of GluN2B currents (40). Aβ-driven synaptic depression was still observed upon incubation with 50 nM PEAQX (Fig. 2 *G* and *H*). These results suggest that inhibition of GluN2B, rather than GluN2A, prevents the effects of oligomeric Aβ. Notably, incubation of slices with these drugs did not depress basal synaptic function (Fig. S1). This indicates that the block of Aβ-driven synaptic depression by these drugs is not an occlusion type effect.

Aβ-Driven Synaptic Depression Is Independent of Ion Flux Through the NMDAR. Several forms of synaptic plasticity depend on Ca^{2+} flux through NMDARs (31, 32, 41). To investigate whether ion flux through GluN2B-containing NMDARs is required in Aβ-mediated synaptic depression, slices were incubated at the time of APP-CT100 viral infection with either 30 μM MK-801 or 200 μM ketamine. Notably, cells expressing APP-CT100 in the presence of these NMDAR ion-channel blockers displayed synaptic depression that was similar to that seen with no drug (MK-801 vs. no drug: $P = 0.8$; ketamine vs. no drug: $P = 0.4$; Fig. 3 *A* and *C*) and significantly different from the effects of GluN2B antagonists (MK-801 vs. Ro 25-6981: $P = 0.002$; ketamine vs. Ro 25-6981: $P = 0.02$). Because MK-801 and ketamine are use-dependent, we conducted control experiments to ensure that the majority of synaptic NMDARs were blocked within the time when Aβ begins to be expressed in the infected organotypic slices (∼8 h). Slices were incubated in MK-801 for different periods of time and measured NMDAR-mediated charge transfer, normalized by AMPAR-mediated charge transfer. After 4 h of MK-801 exposure, NMDAR-mediated charge transfer was 4% of that seen in the absence of the drug (Fig. S2). Note that this block of ion flux through synaptic NMDARs by MK-801 is considerably greater than that provided by GluN2B antagonists (because the latter do not block GluN2A-containing NMDARs, which provide ∼20% of NMDAR-mediated current in our tissue). Thus, although the activation of GluN2B-type NMDARs is required for Aβ-mediated synaptic depression, ion flux through synaptic NMDARs is not required. Extrasynaptic NMDARs have been proposed to mediate some of the actions of Aβ (16). To test whether ion flux through extrasynaptic NMDARs contributes to Aβ-mediated synaptic depression, we used 100 μM 7 chlorokynurenate (7-CK), which blocks NMDARs at the glycine-binding site. 7-CK effectively blocked both synaptic and extrasynaptic NMDAR-mediated currents [see companion article (35)] but failed to block Aβ-mediated synaptic depression (7-CK vs. no drug: $P = 0.4$; 7-CK vs. Ro 25-6981: $P = 0.001$; Fig. 3 *B* and *C*). These data indicate that NMDAR activation, but not ion flow through the NMDAR, is necessary for Aβ-mediated synaptic AMPAR depression. Combined, our findings suggest that a change in GluN2B conformation is necessary for Aβ-driven signaling to proceed.

Oligomeric Aβ Promotes the GluN2B to GluN2A Switch. Previous studies have identified effects driven by ion channel-independent actions of NMDARs. Endocytosis of NMDARs (36), as well as a switch of GluN2B- for GluN2A-containing synaptic NMDARs (37), can be driven by NMDAR activation and do not require NMDAR ion-channel function. Because Aβ also produces depression of the NMDAR component of transmission (7), we wished to determine whether GluN2A- or GluN2B-containing NMDAR-mediated transmission is reduced by Aβ. We compared NMDAR-mediated transmission in cells expressing APP-CT100 and nearby noninfected neurons, both before and after

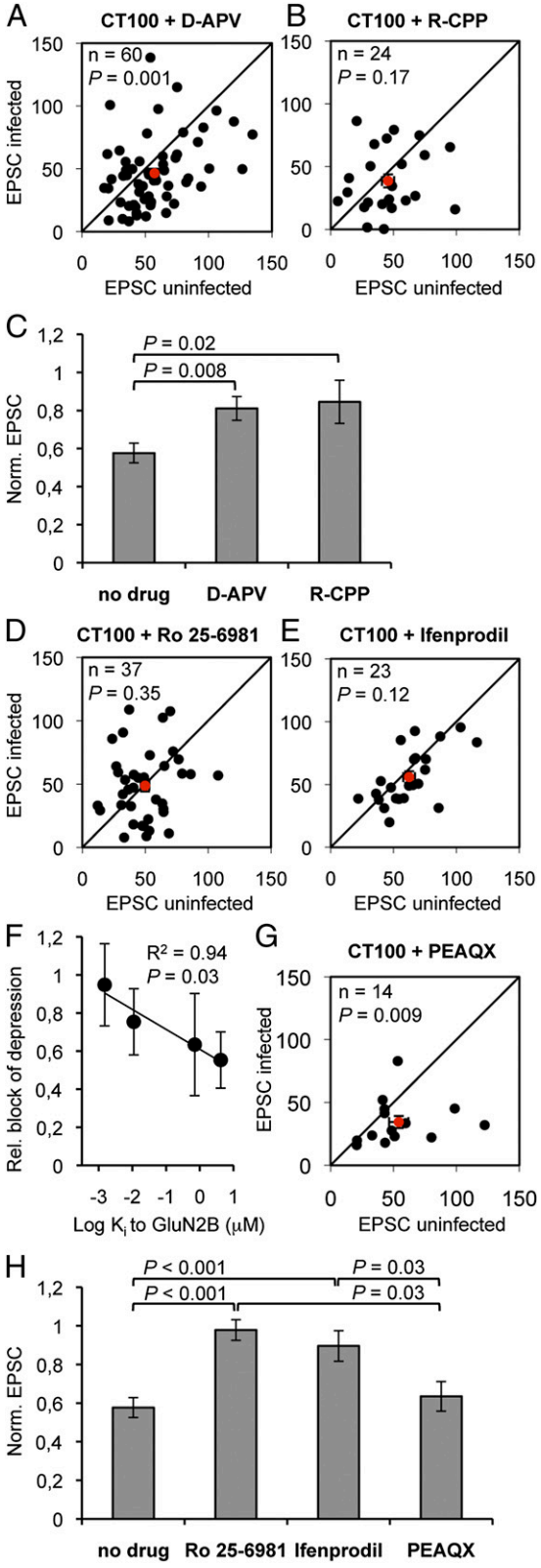

Fig. 2. Oligomeric Aβ-mediated synaptic depression requires GluN2B-containing NMDAR function. (*A*, *B*, *D*, *E*, and *G*) Dot-plots of paired EPSC recordings, average denoted in red. (*C* and *H*) EPSCs of APP-CT100–infected neurons normalized to neighboring uninfected neurons upon incubation with indicated drugs. In slices incubated with 100 μM D-APV (*A*) or with 20 μM R-CPP (*B*) Aβ-driven synaptic AMPAR depression is significantly inhibited (*C*). Incubation with GluN2B-selective antagonists 3 μM Ro 25-6981 (*D*) or 30 μM ifenprodil (*E*) effectively blocked synaptic AMPAR depression in APP-CT100–expressing neurons. (*F*) For the four GluN2-specific drugs as shown in *A*–*E*, their capacity to block the Aβ-mediated synaptic depression was plotted vs. their affinity (K_i) for GluN2B. (*G*) PEAQX (50 nM) did not block Aβ-driven synaptic AMPAR depression. (*H*) Bar graphs and statistical comparisons for data shown in dot-plots. Error bars, SEM. Statistics: paired Student *t* test of log-transformed data (*A*, *B*, *D*, *E*, and *G*), nonpaired Student *t* test (*C* and *H*), and regression analysis (*F*).

addition of 3 μM Ro 25-6981, the antagonist to GluN2B. (We note that wash-in with Ro 25-6981 did not affect AMPAR-mediated synaptic transmission in APP-CT100 infected neurons, after such acute addition; Fig. S3.) GluN2B-mediated NMDAR responses were significantly reduced in neurons expressing APP-CT100 (Fig. 4 *A* and *B*). However, GluN2A-mediated responses, as measured by the current remaining after Ro 25-6981, did not differ between cells expressing APP-CT100 and nonexpressing cells. As a result, the ratio of GluN2A to GluN2B increased after exposure to Aβ-oligomers (Fig. 4*C*). To assess whether these NMDAR subunit-specific effects depended on ion flux through its channel, hippocampal slices were incubated with either 100 μM D-APV or 200 μM ketamine. (The measurement of NMDAR currents in this experiment restricted us to the use of drugs whose NMDAR binding is fully and rapidly reversible.) The increase in GluN2A to GluN2B ratio was dependent on GluN2 function (no drug vs. D-APV: $P = 0.01$; Fig. 4*C*) but not on ion flux through the NMDAR channel (no drug vs. ketamine: $P = 0.08$; Fig. 4*C*). These results suggest that oligomeric Aβ induces GluN2B–GluN2A switching by selectively removing GluN2B-containing NMDARs from synapses in a manner that requires GluN2B function but not ion-channel function.

Discussion

Here we have examined the mechanism by which the NMDAR contributes to the synaptic depression produced by oligomeric Aβ. It was previously shown that the selective blockade of GluN2B-containing NMDARs could mitigate the effects of Aβ (15, 16, 18, 19). In line with these studies, we find that the Aβ-mediated synaptic AMPAR depression depended on GluN2B activation. Although NMDAR-dependent long-term depression (LTD) is thought to require calcium ion flow through the NMDAR [(42–44); but see companion article in this issue for an opposing view (35)], the Aβ-driven synaptic AMPAR depression was independent of NMDAR ion flux. These data indicate that Aβ action on synaptic transmission requires an unconventional, metabotropic type of NMDAR signaling. One possibility is that Aβ, or a signaling molecule activated by Aβ, binds to GluN2B, leading to a conformational change of the NMDAR that transmits the signal to downstream effectors. It is also possible that a GluN2B-dependent process (e.g., a GluN2B-binding protein whose synaptic presence/activity requires ligand-driven conformational changes of GluN2B) is necessary for oligomeric Aβ-driven signaling to proceed. We note that the concentrations of NMDAR antagonists used in Fig. 2 are considerably above the K_d values for binding to the NMDAR. Additionally, the differences in the drug's ability to block synaptic depression are likely due to the drug's ability to block a conformational change in the NMDAR subunit. This suggests that the affinity of the drug for NMDAR subunit (and not only the fractional occupancy at the inhibitory site) is related to its ability to block a conformational change that transmits the metabotropic signal.

In addition to a loss of synaptic AMPARs, oligomeric Aβ signaling also leads to a reduction in synaptic NMDAR currents (6, 7). It is likely that Aβ oligomers remove AMPARs and NMDARs from synapses by targeting a common signaling pathway, because a blockade of AMPAR endocytosis prevents the Aβ-mediated NMDAR depression (6). Our finding that both effects depend on ion flux-independent NMDAR signaling further supports the

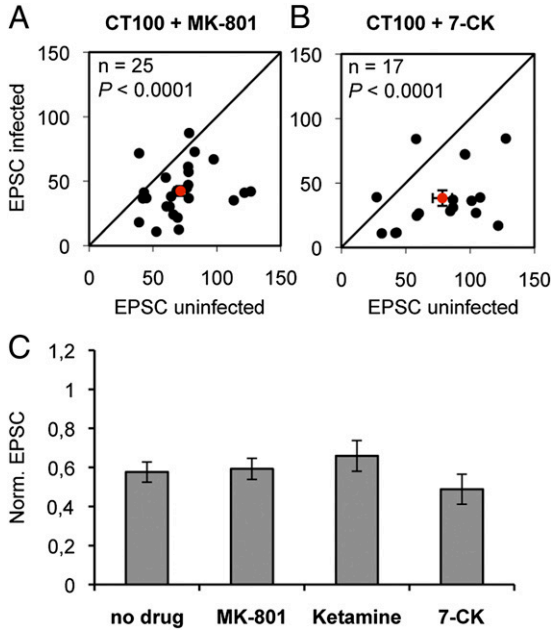

Fig. 3. Oligmeric Aβ-mediated synaptic depression is independent of ion flux through the NMDAR. (*A* and *B*) Dot-plots of paired EPSC recordings, average denoted in red. (*C*) EPSCs of APP-CT100–infected neurons normalized to neighboring uninfected neurons upon incubation with indicated drugs. Incubation with 30 μM MK-801 (*A* and *C*), 200 μM ketamine (*C*), or 100 μM 7-Cl-kynurenate (*B* and *C*) did not block synaptic AMPAR depression in APP-CT100–expressing cells. Error bars, SEM. Statistics: paired Student *t* test of log-transformed data when comparing cell pairs, nonpaired Student *t* test when comparing different conditions.

notion that both these Aβ-mediated effects are functionally linked. We observed that oligomeric Aβ selectively depresses responses from GluN2B-containing NMDARs and not from those that contain GluN2A. It will be interesting to establish whether the GluN2B subunit makes an NMDAR susceptible to Aβ activity or whether GluN2A renders an NMDAR Aβ-resistant. This distinction is relevant in light of the NMDAR subunit composition within synapses of the mature hippocampus. In contrast to the hippocampal synapses of immature age in our model system, mature synapses generally contain low amounts of GluN2B/GluN1 and predominantly contain GluN2A/GluN1 and hetero-trimeric GluN2A/GluN2B/GluN1 receptors (25). GluN2B/GluN1s are expressed in mature neurons but are predominantly located in extrasynaptic regions of the cell membrane (45). A recent study suggests that Aβ oligomers can effect a change through these extrasynaptic GluN2B/GluN1s (16).

A previous study showed that ligand binding to NMDARs led to ion flux-independent endocytosis of NMDARs that is regulated by tyrosine dephosphorylation (36). Although this NMDAR function was only studied for GluN2A-containing NMDARs (36), a similar scenario involving NMDAR dephosphorylation could account for the Aβ-mediated reduction in synaptic GluN2B currents observed here. Indeed, we found that a tyrosine phosphatase inhibitor blocked Aβ-induced depression of AMPAR-mediated transmission (Fig. S4). In line with this scenario, the Aβ-dependent endocytosis of NMDARs requires phosphatase activity, and tyrosine dephosphorylation of GluN2B correlates with GluN1/GluN2B endocytosis (46, 47). Interestingly, EphB2, a receptor tyrosine kinase that selectively controls the synaptic localization and function of GluN2B-containing NMDARs in mature neurons (48), has been implicated in the synapto-toxic effects of Aβ oligomers (8, 49, 50). By binding EphB2 and inducing its degradation (49), oligomeric Aβ could deprive synapses of a process that stabilizes their GluN2B-containing NMDARs. It will be interesting to assess whether a blockade of Aβ–EphB2 interaction will also prevent Aβ-induced AMPAR depression at synapses.

We here show that Aβ oligomers increased the GluN2A to GluN2B ratio by selectively reducing the synaptic currents of GluN2B-containing NMDARs. An increased Aβ production may therefore accelerate the maturation of synapses by promoting a switch of GluN2B- for GluN2A-containing synaptic NMDARs. Increasing the expression levels of GluN2A can also drive an NMDAR subunit switch, and similar to the Aβ-driven effects on synapses, this process requires glutamate-binding to GluN2s but does not require ion flux through the NMDAR (37). Our findings suggest that oligomeric Aβ taps into this ion channel-independent GluN2B signaling to initiate NMDAR subunit switching and

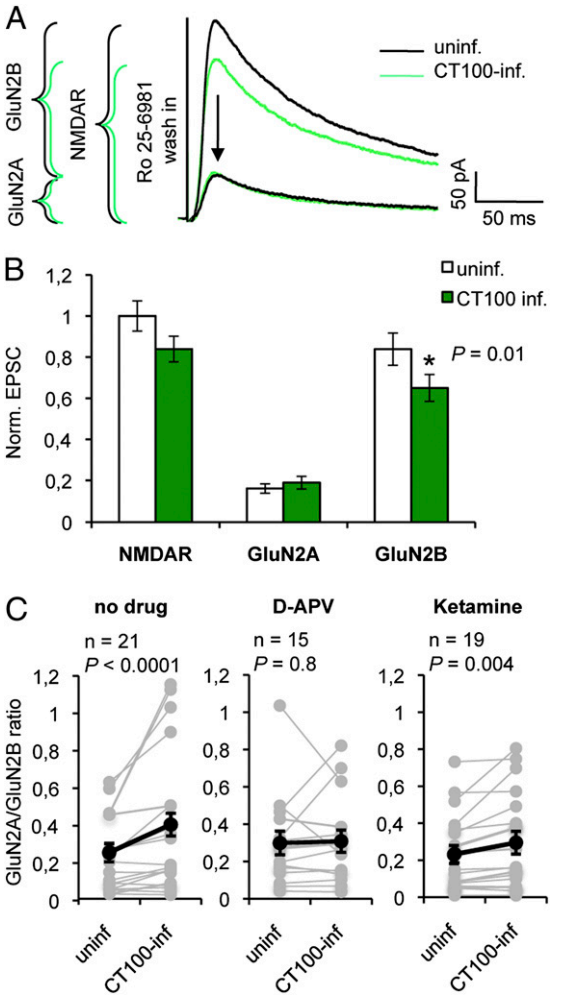

Fig. 4. Oligomeric Aβ selectively reduces GluN2B-mediated synaptic currents and increases the synaptic GluN2A to GluN2B ratio in an ion flux-independent manner. (*A*) Example traces of NMDAR currents from pairs of infected (green) and uninfected (black) CA1 neurons, before and after Ro 25-6981 wash-in to reveal GluN2A- and GluN2B-contributing NMDAR currents. (*B*) Paired NMDAR EPSCs of APP-CT100–infected neurons (green bars), normalized to neighboring uninfected neurons (white bars). (*C*) GluN2A to GluN2B current ratio of pairs of APP-CT100 infected and its neighboring uninfected CA1 neuron, individual pairs in gray, average in black. (*A* and *B*) APP-CT100 expression led to a selective loss in GluN2B currents and increase in GluN2A to GluN2B ratio. Both these effects were inhibited upon incubation of hippocampal slices with 100 μM D-APV during APP-CT100 expression but remained unaffected upon incubation with 200 μM ketamine (*C*). Error bars, SEM. Statistics: paired Student *t* test.

synaptic depression, thereby decreasing the capacity for synaptic plasticity. Identification of the molecular components of this signaling may offer new targets in therapies for Alzheimer's disease.

Materials and Methods

Constructs of APP-CT100 and APP-CT84 were expressed in CA1 neurons in rat organotypic hippocampal slices, using Sindbis virus. Virus was injected into CA1 of 6–13 days in vitro (DIV) slice cultures, and cells were allowed to express for 20–30 h before recording. Slices were incubated in drugs [NMDAR antagonists (Tocris Bioscience) or scyllo-inositol (TCI)] during the 20- 30-h infection period, unless otherwise indicated. Just before recording, a cut was made between CA3 and CA1 to prevent stimulus-induced bursting. Simultaneous whole-cell recordings were obtained from pairs of neighboring control and infected CA1 pyramidal neurons under visual guidance using differential interference contrast and fluorescence microscopy. Two stimulating electrodes, two-contact Pt/Ir cluster electrode (Frederick Haer), were placed between 100 and 300 μm down the apical dendrite, 100 μm apart, and 200 μm laterally in opposite directions. Whole-cell recordings were obtained with Axopatch-1D amplifiers (Molecular Devices) using 3- to 5-MΩ pipettes with an internal solution containing 115 mM cesium methanesulfonate, 20 mM CsCl, 10 mM Hepes, 2.5 mM $MgCl_2$, 4 mM Na_2ATP, 0.4 mM Na_3GTP, 10 mM sodium phosphocreatine (Sigma), and 0.6 mM EGTA (Amresco), at pH 7.25. External perfusion consisted of artificial cerebrospinal fluid containing 119 mM NaCl, 2.5 mM KCl, 4 mM $CaCl_2$, 4 mM $MgCl_2$, 26 mM $NaHCO_3$, 1 mM NaH_2PO_4, and 11 mM glucose (pH 7.4), and gassed with 5% CO_2/95% O_2 at 27 °C with 4 mM $MgCl_2$, 4 mM $CaCl_2$, 4 μM 2-chloroadenosine (Sigma), and 100 μM picrotoxin (Sigma). All recordings were done by stimulating two independent synaptic inputs 1.5 s apart; results from the two pathways were averaged and counted as $n = 1$. The AMPAR-mediated excitatory postsynaptic current (EPSC) was measured as peak inward current at −60 mV. NMDAR-mediated currents were measured as peak outward current at +40 mV in the presence of 3 μM 2,3-dihydroxy-6-nitro-7-sulfamoyl-benzo[*f*]quinoxaline-2,3-dione (NBQX) (Tocris). EPSC amplitudes were obtained from the average of at least 50 sweeps. For measuring the ratio of NMDAR EPSC over AMPAR EPSC (N/A ratio) after incubation with MK-801, the NMDAR EPSCs were determined by measuring the average response of the first five sweeps at + 40 mV, 200–250 ms after evoking a current, and AMPAR EPSCs were subsequently determined by measuring peak responses at +40 mV after addition of 100 μM D-APV (Tocris). Miniature EPSCs were recorded in the presence of tetrodotoxin (Tocris) and picrotoxin. Data were acquired and analyzed using custom software written in Igor Pro (Wavemetrics). Statistical comparisons (*P*) were performed using log-transformed data, paired two-tailed Student *t* test for paired EPSC measurements, and nonpaired two-tailed Student *t* test for comparisons between different sets of experiments.

ACKNOWLEDGMENTS. We thank Irina Hunton and Tessa Lodder for expert technical assistance. R.M. was supported by the National Institutes of Health, the Shiley-Marcos Foundation, and the Cure Alzheimer's Foundation, and H.W. K. by the Internationale Stichting Alzheimer Onderzoek.

1. Terry RD, et al. (1991) Physical basis of cognitive alterations in Alzheimer's disease: Synapse loss is the major correlate of cognitive impairment. *Ann Neurol* 30(4): 572–580.
2. Mucke L, et al. (2000) High-level neuronal expression of abeta 1-42 in wild-type human amyloid protein precursor transgenic mice: Synaptotoxicity without plaque formation. *J Neurosci* 20(11):4050–4058.
3. Shankar GM, et al. (2008) Amyloid-beta protein dimers isolated directly from Alzheimer's brains impair synaptic plasticity and memory. *Nat Med* 14(8):837–842.
4. Lesné S, et al. (2006) A specific amyloid-beta protein assembly in the brain impairs memory. *Nature* 440(7082):352–357.
5. Cheng IH, et al. (2007) Accelerating amyloid-beta fibrillization reduces oligomer levels and functional deficits in Alzheimer disease mouse models. *J Biol Chem* 282(33): 23818–23828.
6. Hsieh H, et al. (2006) AMPAR removal underlies Abeta-induced synaptic depression and dendritic spine loss. *Neuron* 52(5):831–843.
7. Kamenetz F, et al. (2003) APP processing and synaptic function. *Neuron* 37(6): 925–937.
8. Lacor PN, et al. (2007) Abeta oligomer-induced aberrations in synapse composition, shape, and density provide a molecular basis for loss of connectivity in Alzheimer's disease. *J Neurosci* 27(4):796–807.
9. Lambert MP, et al. (1998) Diffusible, nonfibrillar ligands derived from Abeta1-42 are potent central nervous system neurotoxins. *Proc Natl Acad Sci USA* 95(11): 6448–6453.
10. Shankar GM, et al. (2007) Natural oligomers of the Alzheimer amyloid-beta protein induce reversible synapse loss by modulating an NMDA-type glutamate receptor-dependent signaling pathway. *J Neurosci* 27(11):2866–2875.
11. Texidó L, Martín-Satué M, Alberdi E, Solsona C, Matute C (2011) Amyloid β peptide oligomers directly activate NMDA receptors. *Cell Calcium* 49(3):184–190.
12. Ting JT, Kelley BG, Lambert TJ, Cook DG, Sullivan JM (2007) Amyloid precursor protein overexpression depresses excitatory transmission through both presynaptic and postsynaptic mechanisms. *Proc Natl Acad Sci USA* 104(1):353–358.
13. Walsh DM, et al. (2002) Naturally secreted oligomers of amyloid beta protein potently inhibit hippocampal long-term potentiation in vivo. *Nature* 416(6880):535–539.
14. Wang HW, et al. (2002) Soluble oligomers of beta amyloid (1-42) inhibit long-term potentiation but not long-term depression in rat dentate gyrus. *Brain Res* 924(2):133–140.
15. Hu NW, Klyubin I, Anwyl R, Rowan MJ (2009) GluN2B subunit-containing NMDA receptor antagonists prevent Abeta-mediated synaptic plasticity disruption in vivo. *Proc Natl Acad Sci USA* 106(48):20504–20509.
16. Li S, et al. (2011) Soluble Aβ oligomers inhibit long-term potentiation through a mechanism involving excessive activation of extrasynaptic NR2B-containing NMDA receptors. *J Neurosci* 31(18):6627–6638.
17. Liu J, et al. (2010) Amyloid-β induces caspase-dependent loss of PSD-95 and synaptophysin through NMDA receptors. *J Alzheimers Dis* 22(2):541–556.
18. Rammes G, Hasenjäger A, Sroka-Saidi K, Deussing JM, Parsons CG (2011) Therapeutic significance of NR2B-containing NMDA receptors and mGluR5 metabotropic glutamate receptors in mediating the synaptotoxic effects of β-amyloid oligomers on long-term potentiation (LTP) in murine hippocampal slices. *Neuropharmacology* 60(6): 982–990.
19. Rönicke R, et al. (2011) Early neuronal dysfunction by amyloid β oligomers depends on activation of NR2B-containing NMDA receptors. *Neurobiol Aging* 32(12): 2219–2228.
20. Roselli F, Hutzler P, Wegerich Y, Livrea P, Almeida OF (2009) Disassembly of shank and homer synaptic clusters is driven by soluble beta-amyloid(1-40) through divergent NMDAR-dependent signalling pathways. *PLoS ONE* 4(6):e6011.
21. Wei W, et al. (2010) Amyloid beta from axons and dendrites reduces local spine number and plasticity. *Nat Neurosci* 13(2):190–196.
22. Monyer H, Burnashev N, Laurie DJ, Sakmann B, Seeburg PH (1994) Developmental and regional expression in the rat brain and functional properties of four NMDA receptors. *Neuron* 12(3):529–540.
23. Sheng M, Cummings J, Roldan LA, Jan YN, Jan LY (1994) Changing subunit composition of heteromeric NMDA receptors during development of rat cortex. *Nature* 368(6467):144–147.
24. Stocca G, Vicini S (1998) Increased contribution of NR2A subunit to synaptic NMDA receptors in developing rat cortical neurons. *J Physiol* 507(Pt 1):13–24.
25. Rauner C, Köhr G (2011) Triheteromeric NR1/NR2A/NR2B receptors constitute the major N-methyl-D-aspartate receptor population in adult hippocampal synapses. *J Biol Chem* 286(9):7558–7566.
26. Barria A, Malinow R (2005) NMDA receptor subunit composition controls synaptic plasticity by regulating binding to CaMKII. *Neuron* 48(2):289–301.
27. Philpot BD, Cho KK, Bear MF (2007) Obligatory role of NR2A for metaplasticity in visual cortex. *Neuron* 53(4):495–502.
28. Lau CG, Zukin RS (2007) NMDA receptor trafficking in synaptic plasticity and neuropsychiatric disorders. *Nat Rev Neurosci* 8(6):413–426.
29. Foster KA, et al. (2010) Distinct roles of NR2A and NR2B cytoplasmic tails in long-term potentiation. *J Neurosci* 30(7):2676–2685.
30. Morris RG, Anderson E, Lynch GS, Baudry M (1986) Selective impairment of learning and blockade of long-term potentiation by an N-methyl-D-aspartate receptor antagonist, AP5. *Nature* 319(6056):774–776.
31. Tsien JZ, Huerta PT, Tonegawa S (1996) The essential role of hippocampal CA1 NMDA receptor-dependent synaptic plasticity in spatial memory. *Cell* 87(7): 1327–1338.
32. Malenka RC, Nicoll RA (1993) NMDA-receptor-dependent synaptic plasticity: multiple forms and mechanisms. *Trends Neurosci* 16(12):521–527.
33. Newpher TM, Ehlers MD (2008) Glutamate receptor dynamics in dendritic microdomains. *Neuron* 58(4):472–497.
34. Shepherd JD, Huganir RL (2007) The cell biology of synaptic plasticity: AMPA receptor trafficking. *Annu Rev Cell Dev Biol* 23:613–643.
35. Nabavi S, et al. (2013) Metabotropic NMDA receptor function is required for NMDA receptor-dependent long-term depression. *Proc Natl Acad Sci* 110:4027–4032.
36. Vissel B, Krupp JJ, Heinemann SF, Westbrook GL (2001) A use-dependent tyrosine dephosphorylation of NMDA receptors is independent of ion flux. *Nat Neurosci* 4(6): 587–596.
37. Barria A, Malinow R (2002) Subunit-specific NMDA receptor trafficking to synapses. *Neuron* 35(2):345–353.
38. Dasilva KA, Shaw JE, McLaurin J (2010) Amyloid-beta fibrillogenesis: Structural insight and therapeutic intervention. *Exp Neurol* 223(2):311–321.
39. Karakas E, Simorowski N, Furukawa H (2011) Subunit arrangement and phenylethanolamine binding in GluN1/GluN2B NMDA receptors. *Nature* 475(7355): 249–253.
40. Neyton J, Paoletti P (2006) Relating NMDA receptor function to receptor subunit composition: Limitations of the pharmacological approach. *J Neurosci* 25(5): 1331–1333.
41. Collingridge GL, Isaac JT, Wang YT (2004) Receptor trafficking and synaptic plasticity. *Nat Rev Neurosci* 5(12):952–962.
42. Cummings JA, Mulkey RM, Nicoll RA, Malenka RC (1996) Ca2+ signaling requirements for long-term depression in the hippocampus. *Neuron* 16(4):825–833.

43. Mulkey RM, Malenka RC (1992) Mechanisms underlying induction of homosynaptic long-term depression in area CA1 of the hippocampus. *Neuron* 9(5): 967–975.
44. Dudek SM, Bear MF (1992) Homosynaptic long-term depression in area CA1 of hippocampus and effects of N-methyl-D-aspartate receptor blockade. *Proc Natl Acad Sci USA* 89(10):4363–4367.
45. Petralia RS, Al-Hallaq RA, Wenthold RJ (2009) *Biology of the NMDA Receptor*, Chapter 8, ed Van Dongen AM (CRC, Boca Raton, FL).
46. Snyder EM, et al. (2005) Regulation of NMDA receptor trafficking by amyloid-beta. *Nat Neurosci* 8(8):1051–1058.
47. Kurup P, et al. (2010) Abeta-mediated NMDA receptor endocytosis in Alzheimer's disease involves ubiquitination of the tyrosine phosphatase STEP61. *J Neurosci* 30(17): 5948–5957.
48. Nolt MJ, et al. (2011) EphB controls NMDA receptor function and synaptic targeting in a subunit-specific manner. *J Neurosci* 31(14):5353–5364.
49. Cissé M, et al. (2011) Reversing EphB2 depletion rescues cognitive functions in Alzheimer model. *Nature* 469(7328):47–52.
50. Simón AM, et al. (2009) Early changes in hippocampal Eph receptors precede the onset of memory decline in mouse models of Alzheimer's disease. *J Alzheimers Dis* 17(4):773–786.

Supporting Information

Kessels et al. 10.1073/pnas.1219605110

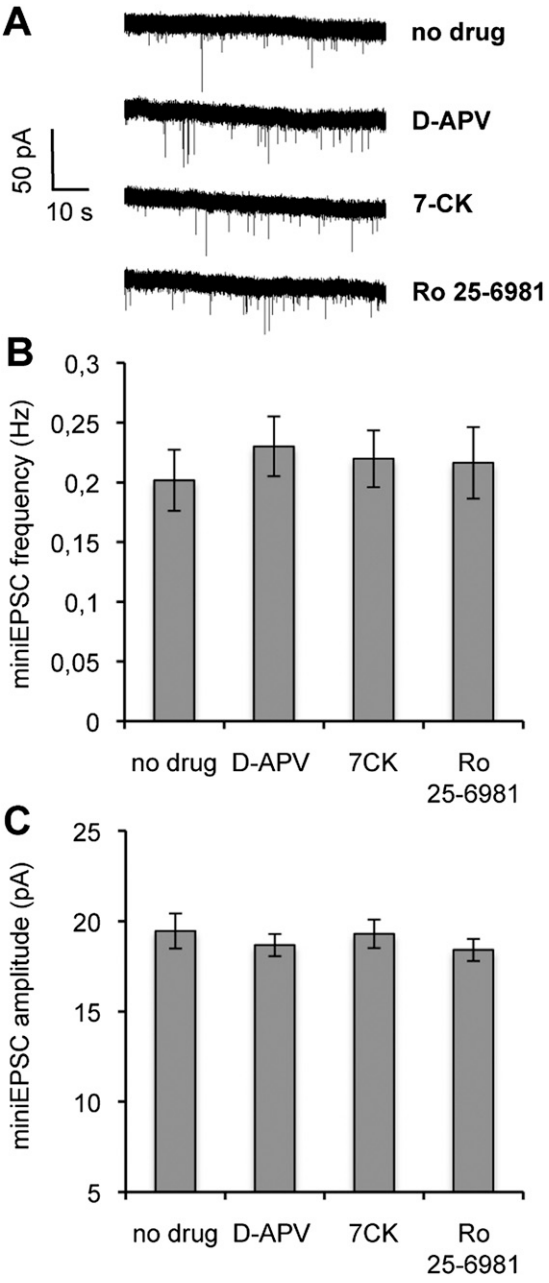

Fig. S1. Incubation of hippocampal slices with NMDA receptor (NMDAR) antagonist does not affect synaptic efficacy. Organotypic hippocampal slices from the same rat were incubated without drug, with 100 μM D-APV, with 100 μM 7-Cl-kynurenate, or with 3 μM Ro 25-6981 for 20–30 h (n = 11 slices per condition). Miniature excitatory postsynaptic currents (mEPSC) were recorded from two CA1 neurons per slice. (*A*) Example traces. (*B*) Average mEPSC frequency, and (*C*) average mEPSC amplitude were calculated. Error bars, SEM.

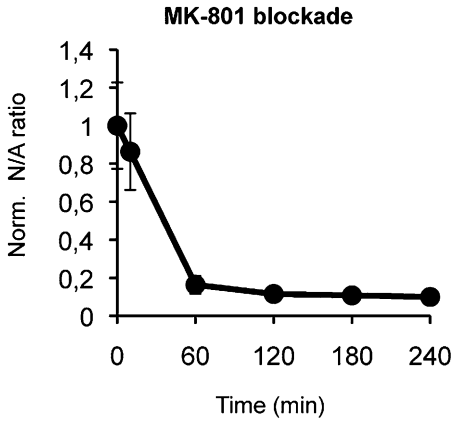

Fig. S2. Time-dependent blockade of NMDARs by MK-801. The ratio of NMDAR EPSC over AMPAR EPSC (N/A ratio) in CA1 neurons was plotted against the time period the organotypic hippocampal slices were exposed to 30 μM MK-801. N/A ratios were normalized to the N/A ratio without MK-801 incubation.

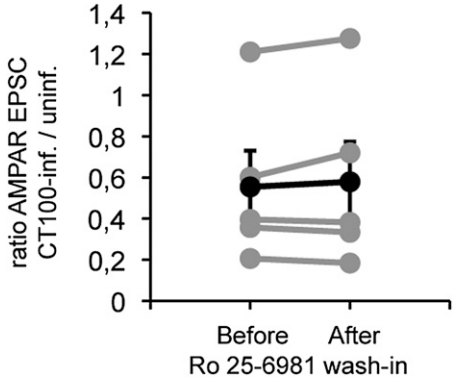

Fig. S3. Acute blockade of GluN2B does not affect Aβ-mediated synaptic depression of AMPAR currents. Paired whole-cell recordings were used to determine the ratio of EPSC from APP-CT100–infected CA1 neurons over EPSC from uninfected counterpart, before and 10–15 min after wash-in of GluN2B antagonist Ro 25-6981 (3 μM). Individual pairs in gray, average denoted in black. Error bars, SEM.

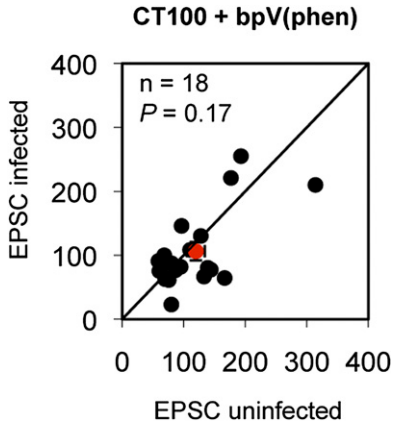

Fig. S4. Oligmeric Aβ-mediated synaptic depression is blocked by tyrosine phosphatase inhibitor. Dot-plot of paired EPSC recordings, average denoted in red. Incubation with 5 μM bpv(phen) blocked synaptic AMPAR depression in APP-CT100–expressing cells.